

# Lasing characteristics of the Ar–Xe and He–Ar–Xe mixtures pumped by fission fragments

Yu.A. Dyuzhov, O.F. Kukharchuk, E.D. Poletaev, V.N. Smolsky, A.A. Suvorov, O.G. Fokina

**Abstract.** The lasing characteristics of the Ar–Xe and He–Ar–Xe mixtures emitting at the transitions of the Xe atom at 1.73 and 2.026  $\mu\text{m}$  upon pumping by fission fragments in the BARS-6 pulsed reactor are studied. We describe an experimental setup and methods for measuring laser beam parameters and characteristics of the active medium of the nuclear-pumped laser in the free-running and master oscillator–amplifier regimes. The dependences of the laser pulse energy on the resonator parameters and the composition and pressure of the working mixture are studied in the free-running regime. A method of modulating the input signal of a single-pass amplifier is proposed for obtaining lasing characteristics of active mixtures. The lasing characteristics of the Ar–Xe and He–Ar–Xe mixtures (the unsaturated gain, saturation intensity, conversion efficiency, etc.) are determined from experiments in the amplifier–oscillator regime and compared with the results reported in other papers.

**Keywords:** nuclear-pumped laser, free-running lasing, single-pass amplifier, input-signal modulation, unsaturated gain, saturation intensity, gas lens.

## 1. Introduction

A promising application of the nuclear energy is its conversion to the laser radiation energy. At present works are under way at the SSC RF IPPE on the development of an energy prototype of a high-power pulsed laser system based on a nuclear-pumped optical quantum amplifier (NPOQA) [1, 2]. This prototype consists of two basic units: the ignition pulsed BARS-6 reactor and a surrounding laser unit. The main components of the NPOQA laser unit are laser active elements (LAEs) filled with a working gas mixture. The problem of a choice of the efficient working mixture for nuclear-pumped lasers was

studied by many authors (see, for example, [3, 4]); however, it still remains of current interest.

The improvement and optimisation of the output energy characteristics of a nuclear-pumped laser – a nuclear-optical energy converter (NOC) – are possible only when reliable information is available on spatiotemporal distributions of active-medium optical parameters such as the unsaturated gain, saturation intensity, attenuation coefficient, and refractive index. Because these important parameters depend on numerous factors including pumping conditions, the laser-mixture partial composition and pressure, and the laser element geometry, their determination with an acceptable accuracy based only on theoretical models seems quite problematic. To solve this problem, it is necessary to perform a variety of calculations and experiments taking into account the specific properties of a particular setup.

In this paper, we present the results of combined experimental and theoretical studies of the NOC operation in the free-running and master oscillator–single-pass amplifier regimes, which allowed us to solve the complex problem of determining the optical parameters of Ar–Xe and He–Ar–Xe media in which efficient lasing was obtained at the transitions in the Xe atom at 1.73 and 2.026  $\mu\text{m}$  upon nuclear pumping. Note that these active media are considered well enough studied, in particular, upon nuclear pumping [4–10]. In a number of cases, lasing with high output characteristics was obtained in small-volume laser cells, the specific output energy achieving  $8 \text{ J L}^{-1}$  and the efficiency of nuclear energy conversion to laser radiation amounting to 3.5%. However, it is very important to perform investigations under pumping conditions close to those inherent in high-power laser systems. Therefore, we used in this study as a laser cell an operating variant of the LAE intended for use in the NPOQA laser unit. Special attention was paid to the determination of the important lasing parameters of a medium such as the unsaturated gain, saturation intensity, conversion efficiency, etc., which are required for the calculation and optimisation of the optical scheme of the NPOQA.

## 2. Study of the lasing characteristics of the Ar–Xe active medium

### 2.1 Experimental setup

The lasing characteristics of the Ar–Xe medium were studied in a BARS-6 two-zone pulsed reactor [11, 12]. Figure 1 presents the scheme of the experimental setup for measuring lasing characteristics of a nuclear-optical energy

Yu.A. Dyuzhov, O.F. Kukharchuk, E.D. Poletaev, V.N. Smolsky, A.A. Suvorov, O.G. Fokina State Scientific Center of the Russian Federation, A.I. Leypunsky Institute for Physics and Power Engineering, pl. Bondarenko 1, 249033 Obninsk, Kaluga region, Russia; e-mail: suvorov@ippe.ru

Received 13 April 2009; revision received 21 August 2009  
*Kvantovaya Elektronika* 40 (1) 11–18 (2010)  
Translated by M.N. Sapozhnikov

converter operating in the free-running regime [13]. Laser active element (3) is placed in polyethylene neutron moderator (2) located at a distance of 680 mm from the centres of active zones of reactors. This LAE represents a thin-wall (0.5-mm thick) stainless steel tube of length 2500 mm and external diameter 49 mm with the inner surface covered with a thin ( $\sim 5\text{-}\mu\text{m}$ ) metal uranium-235 layer applied by the method of magnetron deposition. The ends of the LAE are hermetically sealed with quartz windows with dielectric AR coatings on both surfaces for  $\lambda = 1.73\ \mu\text{m}$ . The LAE is connected to a system for evacuation, filling and purification of the working Ar–Xe mixture.

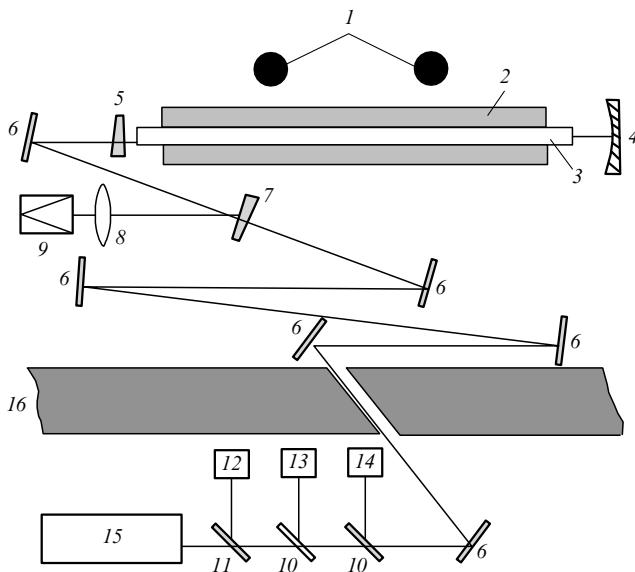


**Figure 1.** Scheme of the experiment: (1) active zones of the reactor; (2) neutron moderator; (3) LAE; (4, 5) resonator mirrors; (6) steering mirrors; (7, 10, 11) beamsplitters; (8) lens; (9) IMO-2N calorimeter; (12) IMO-3 calorimeter; (13, 14) photodetectors; (15) alignment He–Ne laser; (16) concrete wall of the measurement room.

At a distance of 25 cm from the laser-cell ends, resonator mirrors (4) and (5) are located, which are manufactured by the deposition of a dielectric coating on KU-1 quartz substrates. Highly reflecting spherical mirror (4) with the radius of curvature of 10 m and aperture 65 mm had the reflectance  $99.7 \pm 0.2\%$  at the working wavelength ( $1.73\ \mu\text{m}$ ). The reflection coefficient of flat output mirror (5) was changed depending on experimental conditions.

Wedge-shaped beamsplitter (7) divided the laser beam into two parts. A laser beam reflected from mirror (7) was focused by lens (8) on IMO-2N calorimeter (9) measuring the laser pulse energy. A laser beam transmitted through mirror (7) was directed by steering mirrors (6) through a channel in biological protection wall (16) to a measurement room. The total length of the optical path of the scheme was about 15 m. The time characteristics of the laser pulse were recorded with FD9-E111 photodiode (13) and FSB-19 photoresistor (14) on which the laser beam was directed by quartz beamsplitters (10). Additional IMO-3 calorimeter (12) measured the laser beam energy in the measurement room. The resonator and optical scheme were aligned with the help of LG-52 He–Ne laser (15).

The neutron fluence distribution over the LAE length was measured by the method of activation of copper samples which were placed on the LAE surface. The shape of the neutron pump pulse was measured with the help of a vacuum fission chamber containing  $^{235}\text{U}$ , which was placed into the neutron moderator cavity. The energy deposition of fission fragments to the gas medium during a neutron pulse was determined by measuring a pressure jump in the LAE volume with the help of a fast DMI-2 electromagnetic sensor.

## 2.2 Results of measurements and discussion

The lasing characteristics of the Ar–Xe mixture were measured in the free-running regime. Except the possibility of determining the optimal composition and pressure of the working mixture, the analysis of these experiments gives the important characteristics of the active medium such as the stored inversion energy, unsaturated gain, saturation intensity, and the conversion efficiency of nuclear energy to laser radiation energy. We performed about 30 experiments in which the dependences of the laser pulse energy and duration on the transmission of resonator mirrors, the active medium length, the partial composition and total pressure of the working mixture and other parameters were studied.

To determine the conversion efficiency of nuclear energy to laser radiation energy and to obtain the dependences of lasing characteristics of the active medium on the energy deposition, it is necessary to know the amount of energy imparted by fission fragments to a gas medium. In this paper, we determined the energy deposition by measuring a pressure jump in a laser cell during a neutron pulse [14].

By measuring the dependences of laser radiation parameters on the Ar–Xe mixture pressure and partial composition we determined the optimal composition of the mixture (Ar:Xe = 200:1) and its total pressure (0.5 atm). Figure 2 presents the dependence of the laser beam energy  $E_{\text{las}}$  on the transmission coefficient  $T$  of the output mirror of the resonator under these conditions. Note that at mixture pressures above 0.7 atm, the energy deposition to gas from fission fragments does not increase because the fission fragments almost completely lose their energy inside the LAE in the case of medium parameters and cell size used in experiments.

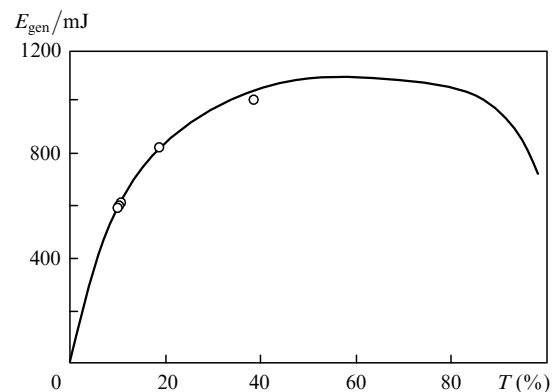


**Figure 2.** Dependence of the laser radiation energy on the transmission coefficient of the output resonator mirror (circles: experiment, curve: calculation).

One can see from Fig. 2 that as the output mirror transmission is increased from 10% to 38%, the output energy of the laser increases up to  $\sim 1$  J. The conversion efficiency of the fission fragment energy to the laser radiation energy is  $\sim 1\%$ . Calculations based on the solution of the one-dimensional radiation transfer equation in the active medium for a plane resonator showed (solid curve in Fig. 2) that the optimal transmission of the output resonator mirror in our case was 40%–60%. Such a high optimal transmission is caused by high intracavity radiation losses due to Fresnel reflection from AEL windows. Although the windows had the AR coating, the residual reflection at a wavelength of  $1.73\ \mu\text{m}$  was 3.5%, which resulted in the increase in intracavity losses by  $\sim 14\%$ .

The unsaturated gain  $\alpha_0$  of the active medium at specific pump powers  $W_{\text{pump}}$  averaged over the LAE volume close to maximal for our experiments (about  $250\ \text{W cm}^{-3}$ ) was determined by the method of calibrated losses. For this purpose, a plate with the known transmission at the working wavelength was mounted inside the resonator at an angle to its axis. Figure 3 presents the dependences of the unsaturated gain on the specific pump power measured in this paper and in papers [5, 7, 8]. One can see that the gain  $\alpha_0 = 2.6 \times 10^{-2}\ \text{cm}^{-1}$  for the average pump power  $W_{\text{pump}} = 220\ \text{W cm}^{-3}$ , which coincides with data obtained in [8] for  $W_{\text{pump}} = 200\ \text{W cm}^{-3}$  and does not contradict results [7] obtained at lower pump powers. It also follows from Fig. 3 that data [5] are not consistent with our results and results obtained in [7, 8].

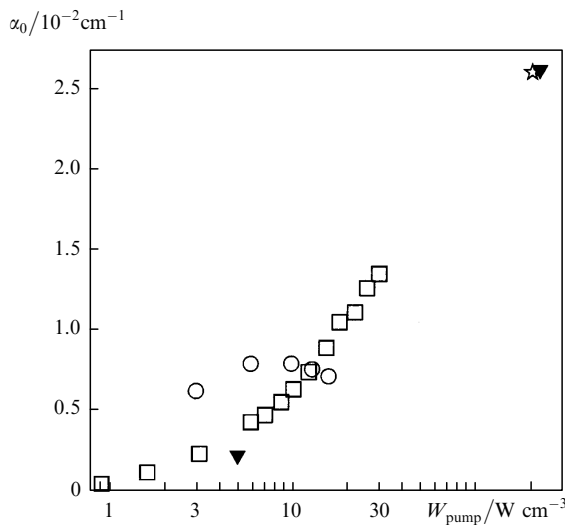


**Figure 3.** Dependence of the unsaturated gain of the Ar–Xe mixture at a wavelength of  $1.73\ \mu\text{m}$  on the specific pump power of fission fragments; data from the present paper ( $\blacktriangledown$ ) and papers [5] ( $\circ$ ), [7] ( $\square$ ), and [8] ( $\star$ ).

An important parameter of the active medium is also the saturation intensity  $I_s$ . This parameter was determined from the Rigrod formula [15] relating the output laser power, the unsaturated gain and saturation intensity with resonator parameters. We found that for  $W_{\text{pump}} = 220\ \text{W cm}^{-3}$  and  $\alpha_0 = 2.6 \times 10^{-2}\ \text{cm}^{-1}$  obtained in our experiments, the saturation intensity of the Ar–Xe medium was  $I_s = 215\ \text{W cm}^{-2}$ . Note that this value of the saturation intensity does not contradict data [7]; however, it is approximately seven times greater than the saturation

intensity obtained in [8], which is, in our opinion, considerably understated.

It is known that the product  $\alpha_0 I_s$  is the limiting value of the stimulated radiation power emitted by the active medium unit volume. Therefore, the maximum efficiency  $\eta_{\text{max}}$  of the laser ('instant' efficiency) can be defined by the expression  $\eta_{\text{max}} = \alpha_0 I_s / W_{\text{pump}}$ . For the power deposition of fission fragments  $W_{\text{pump}} = 220\ \text{W cm}^{-3}$ , we obtain  $\eta_{\text{max}} = 2.5\%$ , in accordance with results [5, 7–9].

Note that the Ar–Xe laser can emit not only at the  $5d[3/2]_1 - 6p[5/2]_2$  transition in xenon at  $1.73\ \mu\text{m}$  studied here, but also at other transitions in xenon, in particular, at the  $5d[3/2]_1 - 6p[3/2]_1$  transition at  $2.026\ \mu\text{m}$ . The transitions responsible for lasing at these two wavelengths have the common upper level. Curves (2) and (3) in Fig. 4 show laser pulses obtained in experiments with output resonator mirrors with transmission coefficients  $T = 38\%$  and  $50\%$  at wavelengths  $1.73$  and  $2.026\ \mu\text{m}$ , respectively, using the Ar:Xe = 200:1 mixture at a total pressure of 0.5 atm. Unlike previous experiments, the energy deposition of fission fragments to the gas volume in these experiments was increased by a factor of 1.6 due to the approach of the laser cell to the reactor. Because the threshold pump power and other laser parameters and their dependences on the specific power deposition are different for these transitions, the temporal distribution of laser radiation exhibits competition between the laser lines. At the beginning of the pump pulse, lasing occurs only at the  $2.026\text{-}\mu\text{m}$  transition [curve (3)] with a low lasing threshold. After lasing at  $1.73\ \mu\text{m}$  begins [curve (2)], the intensity of the first line drastically decreases and then lasing occurs simultaneously at both transitions. At the end of the pump pulse, lasing again is observed only at the  $2.026\text{-}\mu\text{m}$  transition.

Figure 4 also shows that the laser pulse in the case of large energy deposition is considerably shorter than the pump pulse, which considerably reduces the efficiency of nuclear energy conversion to laser radiation. Although the total output energy at both transitions in this experiment was higher than that in previous experiments, achieving 1.5 J, the energy conversion efficiency was only 0.6%. A decrease in the laser pulse duration (or lasing cutoff) in

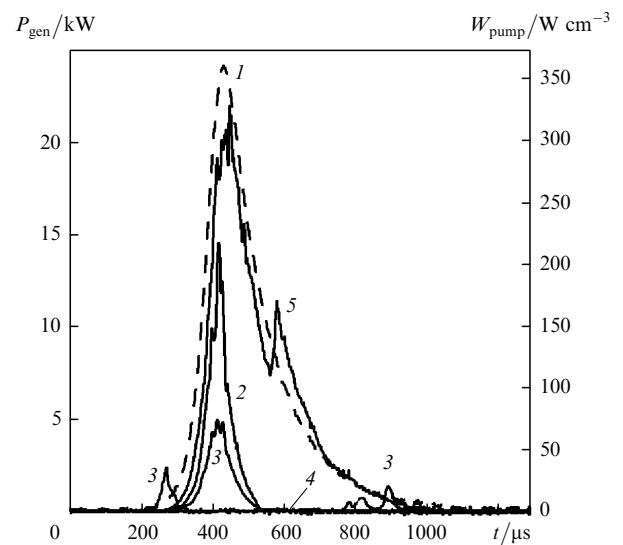


**Figure 4.** Pump (1) and laser pulses at transitions in Xe at  $1.73$  (2, 4) and  $2.026\ \mu\text{m}$  (3, 5) in Ar–Xe (2, 3) and He–Ar–Xe (4, 5) mixtures.

nuclear-pumped Ar–Xe mixtures at large energy depositions was observed in a number of papers [5, 16–20]. This effect has not been explained so far; however, it was found that the lasing cutoff was observed in all the above-mentioned papers at specific energy depositions 80–100  $\text{mJ cm}^{-3}$ , and in our case even at lower energy depositions.

The addition of a small amount of helium to the Ar–Xe mixture leads to an increase in the output power at the 2.026- $\mu\text{m}$  transition, which is explained in a number of papers by a high rate of collision depletion of the lower level of this transition by helium. When a considerable amount of helium is added, lasing at the 1.73- $\mu\text{m}$  transition in Xe ceases at all and lasing is observed only at the 2.026- $\mu\text{m}$  transition. Curves (4) and (5) in Fig. 4 were obtained when the laser cell was filled with the He:Ar:Xe = 1200:400:1 mixture at a total pressure of 1.05 atm. One can see that the 2.026- $\mu\text{m}$  laser pulse [curve (5)] almost completely repeats the pump pulse shape, whereas lasing at 1.73  $\mu\text{m}$  is absent [curve (4)]. The output laser energy was 4.2 J, while the fission fragment energy supplied to the medium, which was measured by a pressure jump, was 250 J. Therefore, the He–Ar–Xe laser efficiency under these conditions is  $\sim 1.7\%$ , which is considerably greater than that for the Ar–Xe mixture.

### 3. Study of lasing characteristics of the He–Ar–Xe mixture

#### 3.1 Experimental setup

We used two LAEs in experimental studies of lasing characteristics of the He–Ar–Xe mixture. One of them was filled with the  $^3\text{He}$ –Ar–Xe mixture and operated in the master oscillator regime, while another, filled with the  $^4\text{He}$ –Ar–Xe mixture, operated in the single-pass amplifier regime. Note that the use of the  $^3\text{He}$ –Ar–Xe mixture in the master oscillator, which is pumped by the products of the nuclear reaction  $^3\text{He} + n \rightarrow ^3\text{H} + p$ , provided a high-quality laser beam [21]. To increase the information content of experiments with the amplifier, we proposed and used the modulation of the master oscillator signal, which expanded the intensity range of the laser beam amplified at different pump powers. This provided the uniqueness and improved

the accuracy of the solution of the inverse problem of reconstruction of medium parameters based on the description of the results of measurements by a theoretical model.

The optical scheme of experiments is presented in Fig. 5. As a master oscillator (MO), we used a laser cell of diameter 49 mm and length 282 cm equipped with output units with Brewster windows. The distance from the MO axis to a straight line passing through the centres of active zones of the BARS-6 reactor was 75 cm. The cell was filled with the working  $^3\text{He}$ –Ar–Xe mixture [21]. In this case, the medium was pumped by the products of the nuclear reaction  $^3\text{He} + n \rightarrow ^3\text{H} + p$ . The MO resonator consisted of highly reflecting dielectric mirror (1) with the radius of curvature 10 m and reflectance 99% at 2.026  $\mu\text{m}$  and output flat mirror (2) with the reflectance 63% at 2.026  $\mu\text{m}$ . The mirrors were mounted at a distance of 10 cm from the Brewster units of the cell, and the resonator length was 330 cm.

As an amplifier we used an LAE with the inner  $^{235}\text{U}$  coating, in which the medium was pumped by the fission fragments of  $^{235}\text{U}$  nuclei. The distance from the LAE axis to a straight line passing through the centres of active zones of the reactor was 65 cm. The LAE amplifier was filled with the  $^4\text{He}$ :Ar:Xe = 600:200:1 gas mixture at a total pressure of 1 atm. Experiments were performed in the BARS-6 pulsed reactor. The neutron pump pulse FWHM was  $\sim 160 \mu\text{s}$ . Under these conditions, the specific peak pump power averaged over the LAE amplifier volume, estimated by measuring a pressure drop, was varied from 160 to 180  $\text{W cm}^{-3}$ . The energy deposition to the MO cell measured by a pressure drop in the working mixture was 34 J ( $7.6 \text{ mJ cm}^{-3}$ ) at a pressure of the  $^3\text{He}$ –Ar–Xe mixture equal to 1 atm, which corresponds to the specific peak pump power  $\sim 45 \text{ W cm}^{-3}$ .

The divergence of a laser beam from the MO was reduced by beam expanding by a factor of 2.3 with the help of a telescope consisting of lenses (3) and (4) and was directed to the LAE amplifier by steering mirrors (5–7) with aluminium coatings. The optical schemes of the amplifier and MO were decoupled with the help of dielectric mirror (8) with the transmission  $T = 1\%$ , which was mounted at the amplifier deposition to attenuate the input signal. In addition, mirror (8) was used as a beamsplitter

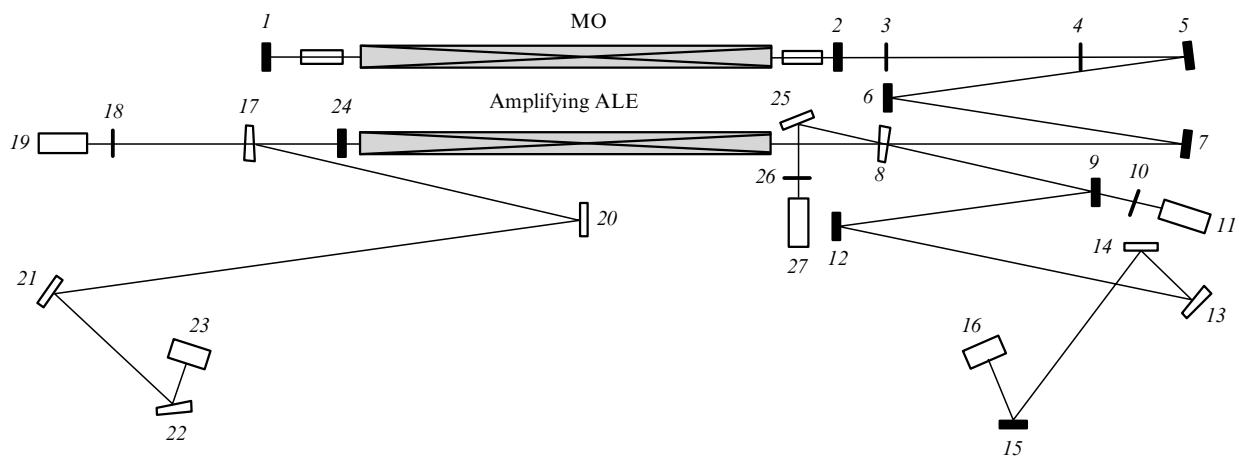


**Figure 5.** Scheme of the experiment: (1, 2, 8, 24) mirrors with dielectric coatings; (3, 4) telescope lenses; (5–7, 12–15, 20–22, 25) steering mirrors with aluminium coatings; (9, 17) beamsplitters; (10, 18, 26) lenses; (11, 19, 27) IMO-2N calorimeters; (16, 23) FSG-22 photoresistor.

and directed the reflected laser beam from the MO to IMO-2N calorimeter (11) measuring the beam energy at the amplifier deposition, and a part of the beam was directed by beamsplitter (9) to the measurement room to measure the pulse shape with FSG-22 photoresistor (16).

An electro-optical FTIR (frustrated total internal reflection) modulator of the MO radiation mounted between telescope lenses (3) and (4) performed periodic attenuation of the laser beam. The laser beam energy at the amplifier output was measured with calorimeter (19) and a small part of the output beam was directed by beamsplitter (17) to the measurement room where the shape of the pulse transmitted through the LAE amplifier was measured with FSG-22 photoresistor (23). Figure 6 presents typical radiation pulses at the amplifier input and output and the pump pulse.

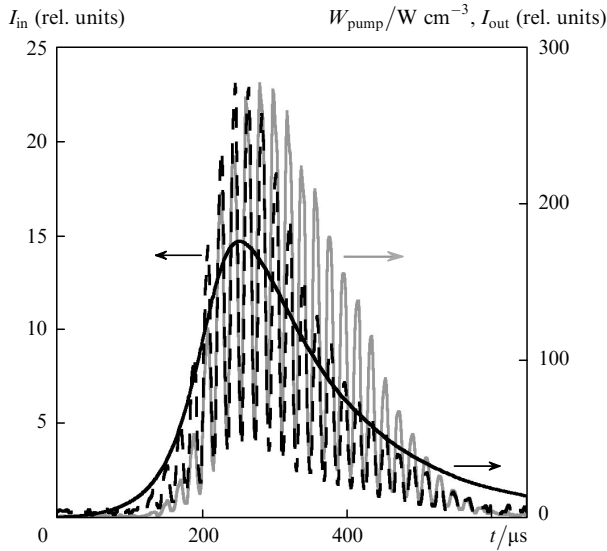


**Figure 6.** Pump ( $W_{\text{pump}}$ ) (solid curve) and radiation intensity pulses at the input ( $I_{\text{in}}$ ) and output ( $I_{\text{out}}$ ) of the amplifier.

### 3.2 Theoretical determination of lasing characteristics of the He–Ar–Xe mixture by the method of modulation of the input signal of a single-pass amplifier

Experimental studies of a nuclear-pumped  $^3\text{He}$  laser showed that the laser-beam divergence was about one milliradian [21]. This exceeds the diffraction divergence limit of the MO beam by an order of magnitude and is caused by the fact that the laser beam in the MO is produced due to the superposition of a great number of statistically independent modes. Because of this, the MO beam is partially coherent and its divergence is determined by the diffraction of radiation on the coherence area proportional to the square of the coherence radius  $\rho_{\text{coh}}$ , which is an order of magnitude smaller than the effective radius of the MO beam.

The propagation of a partially coherent beam through an amplifying element was simulated by solving numerically the equation for the coherence function of radiation in the complex geometrical optics approximation [22] taking into account nonlinear amplification and regular refraction caused by pumping. The gain is  $\alpha_g = \alpha_0/(1 + I/I_s)$  (here  $\alpha_0$  is the small-signal gain,  $I_s$  is the saturation intensity, and  $I$  is the radiation intensity). The regular refraction of the

beam amplified in the LAE was considered in the aberration-free approximation in which the permittivity change is described by the expression  $\Delta\varepsilon(\rho) = \beta^2 \rho^2$  ( $\beta$  is the refraction parameter, and  $\rho$  is the radius vector lying in a plane perpendicular to the LAE axis). We also took into account the spatial inhomogeneities of the unsaturated gain and saturation intensity caused by the inhomogeneous distribution of the specific pump power over the LAE volume and assumed that the refraction parameter  $\beta$  was longitudinally homogeneous and depended on the amplifier-volume-averaged specific pump energy [23].

Based on the qualitative consideration and theoretical estimates of the dependences of optical characteristics of the active medium on the specific local power  $W$  and average pump energy  $E_{\text{pump}}$ , we obtained the following expressions.

The unsaturated gain is described by the expression

$$\alpha_0 = \alpha_0(W) = \alpha_{01} - \alpha_{02} \exp(-W/W_{g1}) - (\alpha_{01} - \alpha_{02}) \exp(-W/W_{g2}), \quad (1)$$

where  $W_{g1}$  is the characteristic specific pump power at which the growth of the unsaturated gain ceases;

$$W_{g2} = (\alpha_{01} - \alpha_{02})W_{g1}/(\eta W_{g1}/I_{s0} - \alpha_{02}) \quad (2)$$

is the threshold specific pump power;  $\eta$  is the local efficiency of the creation of the inverse population of active atoms; and  $I_{s0}$  is the saturation intensity in the mixture in the absence of pumping.

The saturation intensity is

$$I_s = I_s(W) = \eta W/\alpha_0(W). \quad (3)$$

The refraction parameter is

$$\beta = \beta(E_{\text{pump}}) = \left\{ \frac{\beta_0^2}{E_{\beta_0}} \frac{P_0}{10(\gamma - 1)} \times \ln \left[ 1 + \frac{10(\gamma - 1)}{P_0} E_{\text{pump}} \right] \right\}^{1/2}, \quad (4)$$

where  $P_0$  is the initial pressure of the laser mixture (in atm);  $\gamma = 5/3$  is the adiabatic index;  $E_{\beta_0} = 0.031 \text{ J cm}^{-3}$  is the characteristic specific pump energy at which the refraction parameter is equal to  $\beta_0$

The numerical values of coefficients  $\alpha_{01}$ ,  $\alpha_{02}$ ,  $W_{g1}$ ,  $W_{g2}$ ,  $\eta$ ,  $I_{s0}$ , and  $\beta_0$ , entering expressions (1)–(4) are:  $\alpha_0 = 2.17 \times 10^{-2} \text{ cm}^{-1}$ ,  $\alpha_{02} = 1.45 \times 10^{-2} \text{ cm}^{-1}$ ,  $W_{g1} = 145 \text{ W cm}^{-3}$ ,  $W_{g2} = 14.4 \text{ W cm}^{-3}$ ,  $\eta = 0.03$ ,  $I_{s0} = 50 \text{ W cm}^{-2}$ , and  $\beta_0 = 1.75 \times 10^{-3} \text{ cm}^{-1}$ . These values were found by obtaining the best fit between the experimental data and calculations. Because the reconstruction of the optical characteristics of a laser medium is a multiparametric problem and the influence of regular refraction on the propagation of a radiation beam through the LAE should not depend on the presence of active Xe atoms in the mixture, we determined the characteristics of the medium by processing the results of two experimental series.

In the first experimental series, the MO beam was transmitted through an ‘amplifying’ element in which lasing Xe atoms were absent. The processing of the obtained data gave the dependence of the refraction parameter  $\beta$  on the specific pump energy and showed that these experiments could be described by using the model of a partially

coherent Gaussian beam [22] with  $\rho_{\text{coh}} = 0.2$  cm and  $a = 1.74$  cm. In the second series of experiments, the modulated MO beam was transmitted through an amplifying element with Xe atoms. The processing of the results obtained in this series, consisting of four experiments with beams having different modulation depths and different input-beam intensities, gave the dependences of the unsaturated gain and saturation intensity on the local specific pump power.

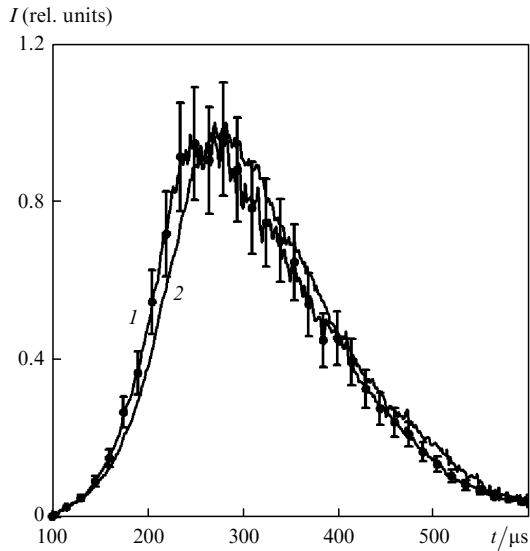


**Figure 7.** Comparison of experimental results (1) and calculations (2) for a medium not containing active Xe atoms.

Figures 7 and 8 present the time dependences of the experimental and theoretical beam intensities transmitted through the amplifying element in the absence and presence of active Xe atoms in it. One can see that the results of calculations are consistent with experimental data.

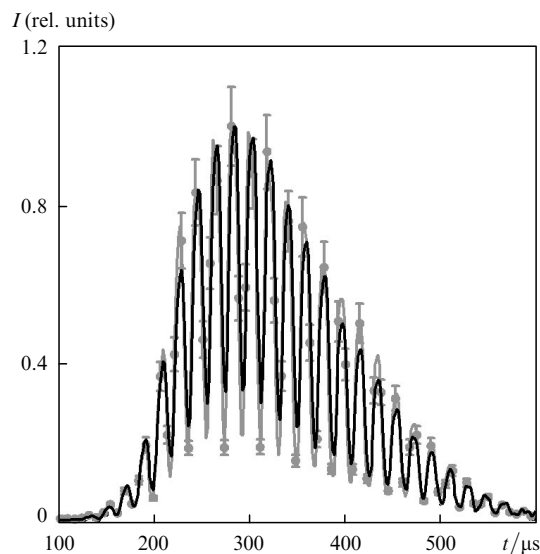


**Figure 8.** Comparison of experimental results (light curves) and calculations (dark curves) for a medium containing active Xe atoms.

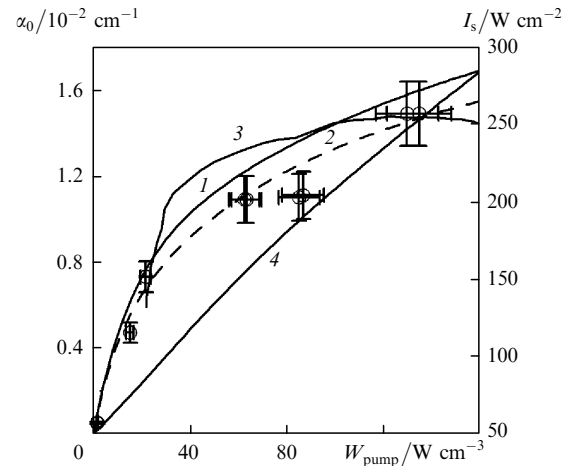


**Figure 9.** Dependences of the unsaturated gain [points and curves (1–3)] and saturation intensity (4) for the He–Ar–Xe mixture at a wavelength of 2.026  $\mu\text{m}$  on the specific pump power obtained in the given paper by the methods of calibrated internal losses (○) and small-signal gain (3), and dependences calculated by expression (1) [the gain averaged over the LAE volume (1) and averaged along the LAE axis (2)] and by expression (3) (4).

Figure 9 presents the dependences of the unsaturated gain  $\alpha_0$  [curves (1) and (2)] and saturation intensity  $I_s$  [curve (4)] on the average specific pump power  $W_{\text{pump}}$ , which were obtained by simulating experiments on modulated signal amplification.

### 3.3 Measurement of the unsaturated gain in the He–Ar–Xe mixture by the small-signal gain method

The aim of the small-signal gain experiment, shown schematically in Fig. 5, was to determine the unsaturated gain in the He:Ar:Xe = 600:200:1 mixture at a total pressure of 1.05 atm by the method different from the modulated-signal amplification method. As a whole, except the absence of a modulator of losses, the experimental scheme and the method of processing of experimental results are the same as in experiments with modulated signal amplification. The dependence of the unsaturated gain on the specific pump power, obtained by the small-signal gain method, is shown in Fig. 9 [curves (3)].

### 3.4 Measurement of the unsaturated gain in the He–Ar–Xe mixture by the method of calibrated intracavity losses

The dependence of the unsaturated gain of the He–Ar–Xe mixture on the specific energy deposition of fission fragments was measured also in the free-running regime by the method of intracavity calibrated losses. The scheme of experiments was similar to that shown in Fig. 1. The experimental method and the method of data processing are described in section 2.2. We studied LAEs filled with the He:Ar:Xe = 1200:400:1 mixture at a total pressure of 1.05 atm. The results of these experiments are presented in Fig. 9 (circles).

### 3.5 Discussion of the results

Figure 9 presents the dependences of  $\alpha_0$  on  $W_{\text{pump}}$  obtained by the method of intracavity calibrated losses (circles), the method of amplification of the modulated signal for the gain averaged over the LAE volume [curve (1)] and the gain averaged over the LAE axis [curve (2)], and by the

small-signal gain method [curve (3)]. One can see that these dependences obtained by three different methods are consistent. One can also see that because of the radial inhomogeneity of the energy deposition, the gain in the axial region of the LAE is somewhat smaller than the volume-averaged gain. Note in addition that the axial gain better agrees with experimental points than the volume-averaged gain. This suggests that the development of lasing begins in the axial region of the LAE. In addition, Fig. 9 shows that the gain tends to saturate with increasing the specific pump power. In accordance with the results of our paper, as follows from (1) and the values of coefficients in (1)–(4) presented above, when the specific pump power considerably exceeds  $W_{g1} = 145 \text{ W cm}^{-3}$ , the unsaturated gain of the He–Ar–Xe mixture tends to the limiting value  $2.17 \times 10^{-2} \text{ cm}^{-1}$ .

Curve (4) in Fig. 9 demonstrated the dependence of the saturation intensity of the  $^4\text{He}$ –Ar–Xe laser mixture on the specific pump power, which was obtained here by the modulated-signal amplification method. One can see that the saturation intensity increases almost linearly with increasing the specific pump power.

Note that among the three methods used in this paper for determining the lasing characteristics, only the modulated-signal amplification method can be used for determining both the unsaturated gain and saturation intensity for specified pumping conditions in one series of measurements.

The dependences of the unsaturated gain and saturation intensity on  $W_{\text{pump}}$  obtained in the present paper are compared in Figs 10 and 11 with results obtained in papers [5] and [6], in which optical characteristics of an atmospheric-pressure nuclear-pumped He–Ar–Xe laser were investigated in detail. The analysis of paper [5] showed that the processing of the results of free-running lasing experiments with different types of resonator mirrors (internal and external) and small-signal gain experiments for the same pumping conditions gave considerably different

dependences of the gain and saturation intensity on the specific pump power. In our opinion, this can be related to the imperfection of the experimental method and data processing. It also follows from Fig. 10 that the dependences of the gain on the specific pump power obtained in small-signal gain experiments [6] and free-running lasing experiments with an external-mirror resonator [5] coincide as a whole and give values that considerably exceed those obtained in the present paper and in free-running lasing experiments [5] with an internal-mirror resonator. It seems that the overstated result in [6] was obtained because the authors used a simplified data processing method (for example, neglected the influence of a gas lens on the characteristics of the detected signal).

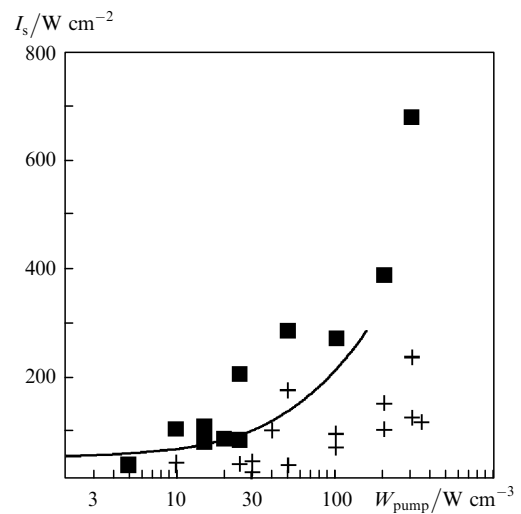


**Figure 11.** Dependences of the saturation intensity of the He–Ar–Xe mixture at a wavelength of  $2.026 \mu\text{m}$  on the specific pump power. Comparison of the results of the present paper with the results obtained in [5]: free-running lasing with external resonator mirrors [5] (+); free-running lasing with internal resonator mirrors [5] (■); modulated signal amplification (present paper) (solid curve).

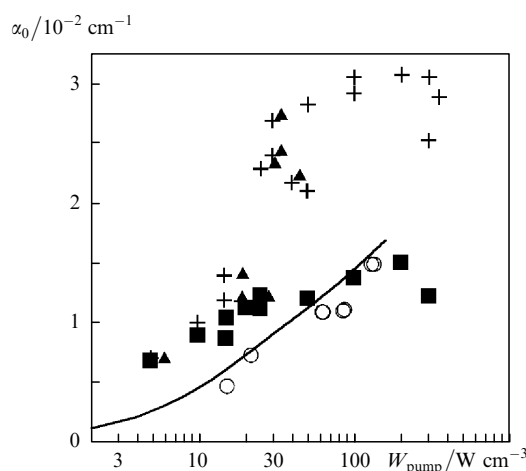


**Figure 10.** Dependences of the unsaturated gain of the He–Ar–Xe mixture at a wavelength of  $2.026 \mu\text{m}$  on the specific pump power. Comparison of the results of the present paper with the results obtained by different methods: free-running lasing with external resonator mirrors [5] (+); free-running lasing with internal resonator mirrors [5] (■); small-signal gain [6] (▲); calibrated intracavity losses (present paper) (○); modulated signal amplification (present paper) (solid curve).

Note in conclusion that we developed the experimental and theoretical method of beam-intensity modulation at the amplifier input and used it to solve the inverse problem for determining the lasing characteristics of the He–Ar–Xe mixture. The dependences of the gain and saturation intensity on the specific pump power obtained by this method are consistent with the corresponding dependences obtained by processing the results of free-running lasing experiments with the NOC. At the same time, conventional simplified data processing methods give contradictory information on lasing characteristics of active media.

## 4. Conclusions

We have studied experimentally and theoretically the lasing characteristics of the Ar–Xe and He–Ar–Xe mixtures pumped by uranium fission fragments.

It was found that, despite the high unsaturated gain and the high energy conversion efficiency, the Ar–Xe mixture cannot be efficiently used at the  $1.73\text{-}\mu\text{m}$  transition in high-power reactor–laser schemes because the energy that can be supplied to it is restricted and the lasing cutoff occurs at high specific energy depositions.

Upon nuclear pumping of the He–Ar–Xe mixture, in which lasing occurs at a wavelength of 2.026  $\mu\text{m}$ , the nuclear energy is quite efficiently converted to the coherent radiation energy, but unlike the Ar–Xe mixture, the lasing cutoff is not observed.

We have proposed the method of modulated signal amplification and used it for the unambiguous determination of optical characteristics of active laser mixtures. By using this method, we found the dependences of the unsaturated gain and saturation intensity on the local specific pump power. These dependences are consistent with the results of processing the independent free-running lasing and small-signal gain experiments.

**Acknowledgements.** This work was supported by the Russian Foundation for Basic Research and the Government of the Kaluga region (Grant No. 07-02-96408).

## References

1. Dyachenko P.P. *Proc. ICENES'96 Conf.* (Obninsk, IPPE, 1996) p. 296.
2. Dyachenko P.P. *Materialy III Mezhdunarodnoi konferentsii 'Problemy lazerov s yadernoi nakachkoi i impul'snye reaktory'* (Proceedings of the III International Conference on Problems of Nuclear-pumped Lasers and Pulsed Reactors) (Snezhinsk: Nuclear Center of the Russian Federation-All-Russian Institute of Technical Physics, 2003) p. 5.
3. *Trudy konferentsii LYaN-92* (Proceedings of the NPL-92 Conference) (Obninsk, Institute of Physics and Power Engineering, 1992); *Trudy konferentsii LYaN-94* (Proceedings of the NPL-92 Conference) (Arzamas-16, All-Russian Research Institute of Experimental Physics, 1994); *Materialy III Mezhdunarodnoi konferentsii 'Problemy lazerov s yadernoi nakachkoi i impul'snye reaktory'* (Proceedings of the III International Conference on Problems of Nuclear-pumped Lasers and Pulsed Reactors) (Snezhinsk: Nuclear Center of the Russian Federation-All-Russian Institute of Technical Physics, 2003).
4. Karelin A.V., Sinyanskii A.A., Yakovlenko S.I. *Kvantovaya Elektron.*, **24**, 387 (1997) [*Quantum Electron.*, **27**, 375 (1997)].
5. Alford W.J., Hays G.N. *J. Appl. Phys.*, **65**, 3760 (1989).
6. Hebner G.A., Hays G.N. *J. Appl. Phys.*, **73**, 3614 (1993).
7. Hebner G.A., Hays G.N. *J. Appl. Phys.*, **73**, 3627 (1993).
8. Magda E.P., Bochkov A.V., Kryzhanovskii V.A., Mukhin S.L. *Trudy konferentsii LYaN-94* (Proceedings of the NPL-92 Conference) (Arzamas-16, 1995) Vol. 1, p. 265.
9. Voinov A.M., Dovbysh L.E., Krivonosov V.N., et al. *Dokl. Akad. Nauk SSSR*, **245**, 80 (1979); *Pis'ma Zh. Tekh. Fiz.*, **7**, 1016 (1981).
10. Abramov A.A., Melnikov S.P., Mukhamatullin A. Kh., et al. *Proc. SPIE Int. Soc. Opt. Eng.*, **5483**, 1 (2004)
11. Dyachenko P.P., Elovskii O.A., Prokhorov Yu.A., et al. Preprint IPPE-2809 (Obninsk, 2000).
12. Dyachenko P.P., Elovskii O.A., Prokhorov Yu.A., et al. *Atom. Energy*, **88**, 337 (2000).
13. Dyachenko P.P., Dyuzhev Yu.A., Kukharchuk O.F., et al. Preprint IPPE-3044 (Obninsk, 2005).
14. Dyachenko P.P., Gamalii A.F., Gulevich A.V., et al., in *Izbrannye trudy Fiziko-energeticheskogo instituta, 1997* (Selected Works of the Institute of Physics and Power Engineering, 1997) (Obninsk: SSC RF-IPPE, 1999) p. 114.
15. Rigrod W.W. *IEEE J. Quantum Electron.*, **14**, 377 (1978).
16. Barysheva N.M., Bochkov A.V., Bochkova N.V., et al. *Trudy konferentsii LYaN-92* (Proceedings of the NPL-92 Conference) (Obninsk, 1992) Vol. 1, p. 374.
17. Konak A.I., Melnikov S.P., Porkhaev V.V., Sinyanskii A.A. *Laser Part. Beams*, **11**, 4 (1993).
18. Batyrbekov E.G., Poletaev E.D., Suzuki E., Miley G.H. *Proc. LIRPP'93 Conf.* (Monterey, CA: AIP Press, 1994) p. 515.
19. Mavlyutov A.A., Mis'kevich A.I., Salamakha B.S. *Trudy konferentsii LYaN-94* (Proceedings of the NPL-94 Conference) (Arzamas-16, 1992) Vol. 1, p. 318.
20. Bokhovko M.V., Budnik A.P., Dobrovol'skaya I.V., Kononov V.N., Kononov O.E. *Pis'ma Zh. Tekh. Fiz.*, **24**, 16 (1998).
21. Dyachenko P.P., Dyuzhov Yu.A., Kukharchuk O.F., et al. Preprint IPPE-3063 (Obninsk, 2005).
22. Gulevich A.V., Evtodiev D.V., Kukharchuk O.F., Suvorov A.A. *Kvantovaya Elektron.*, **35**, 1003 (2005) [*Quantum Electron.*, **35**, 1003 (2005)].
23. Poletaev E.D., Golovchenko S.A., Dyuzhov Yu.A., et al. *Trudy regional'nogo konkursa nauchnykh proektov v oblasti estestvennykh nauk* (Proceedings of the Regional Competition of Scientific Projects in the Field of Natural Sciences) (Kaluga: Poligraf-inform, 2004) Vol. 6, p. 173.